The influence of dune lee side shape

Alice Lefebvre [1], Julia Cisneros [2]

[1]MARUM – Center for Marine Environmental Sciences, University of Bremen, Bremen, Germany
[2]Department of Geological Sciences, Jackson School of Geosciences, UT Austin, Austin, TX 78712, USA

5   *Correspondence to*: Alice Lefebvre (alefebvre@marum.de)

Abstract. Underwater dunes are found in various environments with strong hydrodynamics and sandy, movable sediment such as rivers, estuaries and continental shelves. They have a diversity of morphology, ranging from low to high-angle lee sides, and sharp or rounded crests. Here, we investigate the influence of lee side morphology on flow properties (time-averaged velocities and turbulence). To do so, we carried out a large number of numerical simulations of flows over dunes with a variety

10   of morphologies using Delft3D. Our results show that the value of the mean lee side angle, as well as the value and position of the maximum lee side angle, have an influence on the flow properties investigated. We propose a classification with 3 types of dunes: (1) low-angle dunes (mean lee side < 10°), over which there is no permanent flow separation, except if the maximum slope is steeper than 20° and situated close to the trough, and over which only little turbulence is created; (2) intermediate-angle dunes (mean lee side 10-20°) over which there is generally no permanent but likely an intermittent flow separation,

15   situated over the trough; and (3) high-angle dunes (mean lee side > 20°) over which the flow separates at the brink point and reattaches shortly after the trough, and over which turbulence is high. We discuss the implications of this classification on the interaction between dune morphology and flow.

1 Introduction

Underwater dunes are observed in many shallow and deep-water environments, such as rivers, estuaries, tidal inlets, continental

20   shelves and slopes. They form in systems with beds composed of sediment ranging from coarse silt to fine gravel where the hydrodynamics are strong enough to produce sufficient bedload transport. Until recently, most studies focussed on so-called "high-angle dunes" which possess a steep lee side with slopes of around 30°. These dunes commonly form in small rivers and in flumes (Naqshband et al., 2014; Van Der Mark et al., 2008). Over such dunes, flow separation and recirculation over the lee side produces a turbulent wake and induces bedform roughness. However, many dunes have recently been observed to be

25   "low-angle dunes" with lee side angles much lower than the angle-of-repose. Over low-angle dunes, flow separation is absent or intermittent, and turbulence and roughness are lower than over high-angle dunes (Kwoll et al., 2016; Lefebvre and Winter, 2016). In large rivers, mean lee side angles are commonly between 5 and 20° (Cisneros et al., 2020). This is illustrated in Figure 1 by data from the Mississippi and Waal Rivers which had the steepest and gentlest mean lee side slopes of the six rivers investigated by Cisneros et al. (2020). Bedform lee sides in tidal environments are also often low, with typical values of

30   5 to 20° (e.g. Lefebvre et al., 2021, Figure 1c; Dalrymple and Rhodes, 1995; Franzetti et al., 2013). In addition, contrary to previous simplifications of lee side shape, the lee side is rarely a straight line but rather made of several steeply and gently

sloping portions (Lefebvre et al., 2016). Typically, a comparatively steep slope is observed somewhere along the lee side with gentler slopes towards the crest and/or the trough. The steep slope is often referred to as the "slip face" as sediment is thought to avalanche or slip over this part of the lee side. Here, we refer to this slope as the "steep portion" in an effort to not make any

35 assumption on the type of sediment transport along the dune lee side (see also Lefebvre et al., 2021). The maximum lee side angle value and position can be used to characterise the steep portion characteristics. In large rivers, the maximum lee side angle is generally less than the angle-of-repose (e.g. Figure 1a and b), with an average maximum lee side angle calculated by Cisneros et al. (2020) of 20.5°. In constrained tidal environments (e.g. estuaries and tidal inlets), maximum lee side angles are usually less than 20° (Lefebvre et al., 2021; Prokocki et al., 2022; Dalrymple and Rhodes, 1995) (Figure 1c). In marine

40 environments, there has not yet been a systematic report of mean or maximum angles, in part due to the lack of consistent high-resolution data which may be used to precisely calculate the maximum slope. Nevertheless, it is likely that marine dunes have a variety of mean and maximum lee side angles. Their value is going to vary depending on dune asymmetry, the absolute and relative strength of ebb and flood currents, the influence of other currents (e.g. river flows, wave-related currents), sediment size and tidal phase. In any case, it should be noted that in tidal environments, flow reverses from one tidal phase to the next

45 however large dunes usually stay oriented in one direction during the whole tidal cycle. Therefore, in case of asymmetric bedforms, lee side may be steep during one tidal phase and gentle during the following tidal phase. As a result, a wide range of mean and maximum lee side angles are likely to be found in marine environments.

Interestingly, the shape of river and estuarine dunes differ (Figure 1). River dunes have their steepest slope close to the trough and a rounded crest (Cisneros et al., 2020), whereas estuarine dunes have their steepest slope close to the crest and a sharp

50 crest (Dalrymple and Rhodes, 1995; Lefebvre et al., 2021; Prokocki et al., 2022). Lefebvre et al. (2021) suggested that this is created by the difference in sediment transport direction (Figure 1): in rivers, sediment is systematically eroded from the crest and deposited over the lee side by the unidirectional currents, creating a rounded crest; in estuaries and other tidal environments, sediment at the crest is being mobilised at each tidal phase but only for a short time in each direction resulting in the sharp crest morphology. In open marine environments, various morphologies are found, from sharp to round crests (Van

55 Landeghem et al., 2009; Zhang et al., 2019). Therefore, the difference in dune shape is not strictly reflecting the difference between river and tidal environments, but rather the complex interaction between dune morphology, sediment properties and hydrodynamics. It is therefore likely that a range of shapes are found depending on these specific morphodynamic conditions. The influence of lee side morphology and how it fits within the coupling of feedbacks in the morphodynamic triad has not yet been systematically studied. The aim of this work is therefore to characterise flow properties (velocities and turbulence) over

60 low and high-angle dunes with their steepest slope close to the crest and close to the trough using numerical experiments. We hypothesise that the presence, size and length of the flow separation and turbulent wake vary depending on the value and position of the maximum angle along the lee side.
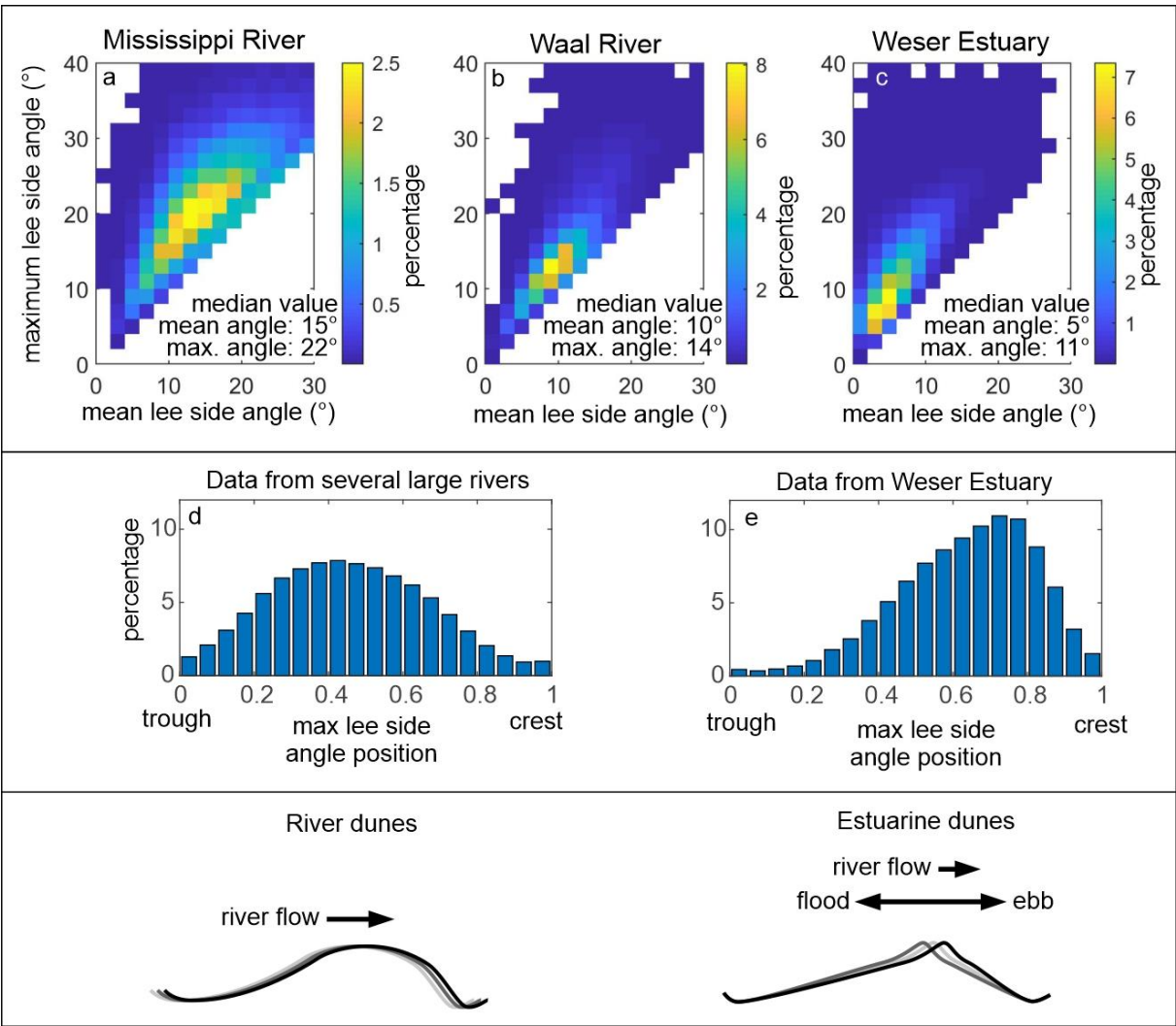
Figure 1. Upper panel: mean and maximum lee side angles from dunes found in the Mississippi and Waal Rivers (data from Cisneros et al., 2020) and the Weser Estuary (data from Lefebvre et al., 2021). Middle panel: histogram of the position of the maximum lee side angle in several large rivers (data from Cisneros et al., 2020) and in the Weser Estuary (data from Lefebvre et al., 2021). Lower panel: schematic representation of the shape of dunes in large rivers and estuaries (after Lefebvre et al., 2021)

2 Methods

2.1 Model description

Delft3D (Deltares, 2014) is a process-based open-source integrated flow and transport modelling system. In Delft3D-FLOW the 3D non-linear shallow water equations, derived from the three-dimensional Navier-Stokes equations for incompressible

free surface flow, are solved. In order to capture non-hydrostatic flow phenomena such as flow separation and recirculation on

75   the lee of dunes, the non-hydrostatic pressure can be computed by using a pressure correction technique: for every time step, a hydrostatic step is first performed to obtain an estimate of the velocities and water levels; a second step, taking into account the effect of the non-hydrostatic pressure, is carried out to correct the velocities and water levels such that continuity is fulfilled (Deltares, 2014).

The Delft3D modelling system has been used to ~~setup~~ set up a two-dimensional vertical (2DV) numerical model using the non-

80   hydrostatic pressure correction technique to simulate horizontal and vertical velocities, turbulent kinetic energy (TKE) and bed shear stresses above fixed bedforms. The model has been calibrated and validated against laboratory flume experiments over idealised high-angle dunes (Lefebvre et al., 2014a) and verified against field data over natural tidal dunes (Lefebvre et al., 2014b). The same numerical model was used here to simulate flow over dunes with varying morphologies. The simulations were performed on a 2DV plane Cartesian model grid over a fixed bed (i.e. no sediment transport) composed of 10 similar

85   bedforms. The following conditions were prescribed constant in time at the lateral open boundaries of the model domain: a logarithmic velocity profile at the upstream boundary, and a water surface elevation of 0 m at the downstream boundary. The bed roughness was set as a uniform roughness length $z_0 = 0.0001$ m. The dune height and length, the water depth and the vertical and horizontal grid size were kept similar for all simulations. The horizontal grid size was set as dx = 0.09 m (271 grid point per dune). A non-uniform vertical grid size, stretched in the vertical direction with fine spacing near the bed (dz1) and

90   coarser spacing in the water column (dz2), was used; dz1 = 0.044 m between the trough position and the height of the crest + 5 dz1, which gradually increased to dz2 = 0.48 m within the remaining water column resulting in 42 layers being used in each simulation. The time step was set to 0.0005 min following a Courant Friedrich Lewy criterion CFL = dt $\sqrt{(g\ h)}$ / dx < 10, where dt is the time step, g is the acceleration due to gravity and h is the water depth. Since the z-model was used, the following condition also applies: dt $\leq$ dx / |u| where |u| is a characteristic value of horizontal velocities (Deltares, 2014). A uniform

95   background horizontal viscosity of 10^{-3} m^2 s^{-1} and background vertical eddy viscosity of 0 m^2 s^{-1} were set. A k-ε turbulence closure model (Uittenbogaard et al., 1992) was used.

2.2. Model experiments

A total of 88 simulations (Table 2) were carried out to test the influence of lee side morphology on flow velocities, separation

100   zone, turbulent kinetic energy and bed shear stress. For all simulations, bedform height (H_b = 0.89 m) and length (L_b = 24.4 m), water depth (h = 8 m) and mean flow velocity (0.8 m/s) were kept similar. The values were chosen based on typical dune dimensions in large rivers (Cisneros et al., 2020). The stoss side followed a cosine shape and the lee side was made of either a line (straight lee side) or three lines (complex lee side) (Figure 2). The straight lee side experiments were made with lee side angles varying from 5° to 30°, in increments of 5°. For each mean lee side angle, simulations were done with the lee side

105   composed of three segments: a steep portion where the maximum angle was fixed (Table 2) and upper and lower lee sides which had angles adjusted so that the mean angle would be between 5 and 30°, in increments of 5°. The steep portion height

was one third of the bedform height ($H_{sf} = H_b / 3 = 0.3$ m). For each maximum lee side angle, 4 configurations were tested, with the position of the steep portion varying from close to the crest to close to the trough (Figure 2).

A distinction was made between sharp profiles and smooth profiles. For some experiments (sharp profiles), the bed profiles

110   were left as created with a cosine stoss side and 1 or 3 straight lines for the lee side, with sharp variations between each section. However, most experiments were made with smooth profiles in order to mimic natural slopes: the profiles were first created from straight lines, and then smoothed using a 5-point smoothing averaged window. The smoothing produced mean angles that were lower than what was set up (Table 2). However, the maximum angle was not smoothed and stayed at the given value (Figure 2).

115

2.3. Model output analysis

From the simulation results, the horizontal and vertical velocities and the TKE above the 7th bedform (from a total of 10 bedforms) are investigated. The position and size of the flow separation zone, when present, is calculated following the method detailed in Lefebvre et al. (2014a): the flow separation line delimitates the region in which the flow going upstream (i.e.

120   negative horizontal velocity) is compensated by flow going downstream. The length of the flow separation zone is the horizontal distance between the separation point and the reattachment point. The relative flow separation length is the flow separation length divided by the dune height. Because Delft3D uses the Reynolds-averaged Navier–Stokes equations, it is not possible to model intermittent flow separation zone; only permanent flow separation can be simulated and is considered here. The shear layer is visualised as a high vertical gradient of streamwise velocity (du/dz) reflecting a rapid change in velocity

125   between two flow regions (Kwoll et al., 2016; Venditti, 2007).

The mean and maximum TKE over the 7th bedform are computed as indicators of the overall turbulence produced and dissipated over each dune shape. In the literature, the wake over bedforms has been defined in different ways: following definitions of wake behind cylinders, as a momentum deficit (i.e. reduced velocity) downstream of the bedform crest (Wiberg and Nelson, 1992; Nelson et al., 1993; Maddux et al., 2003) or by its position, i.e. a specific height or water depth (e.g. 0.1 to

130   0.5 depth), often in cases when velocity profiles are not available at high resolution above the bedforms (Mclean et al., 1994; Bennett and Best, 1995; Mclean et al., 1999). More recently, the wake has been defined as a region of high turbulence, using turbulence intensity and TKE above a constant threshold value (Venditti, 2007), TKE more than 70% of the maximum TKE (Lefebvre et al., 2014a; Lefebvre et al., 2014b), high Reynolds shear stress (Kwoll et al., 2016), or percentage of quadrants 2 and 4 events (Unsworth et al., 2018). In the present work, we define the wake also based on turbulence and therefore will refer

135   to it as "turbulent wake". The turbulent wake is the region where TKE is more than twice the average TKE above a flat bed with similar hydrodynamic conditions. For this, a simulation was carried out with a flat bed (depth 8 m) but all other parameters (e.g. domain length, boundary conditions, roughness length etc.) kept similar to the simulations with dunes. The average TKE for this flat bed simulation is 0.0019 m^2/s^2 and therefore, a threshold value of 0.0038 m^2/s^2 was used to outline the contour of

the wake in the dune simulations. As in previous work, this definition lacks a physical basis as the threshold value is defined

140   quite arbitrarily. However, the turbulent wake contour above straight angle-of-repose dunes corresponds well to what is

expected from the literature and it allows us to highlight changes in TKE intensity and spatial distribution between the different

configurations. The length of the wake is calculated as the horizontal length between the beginning and the end of the wake.

The bed shear stress is calculated by Delft3D using the law of the wall (Deltares, 2014). In the z-layer, strong variations of the

vertical cell size affect the calculation of the bed shear stress. In order to improve accuracy and smoothness of the computed

145   bed shear stress, the local remapping of near-bed layer is used (Platzek et al., 2014). However, due to the high resolution of

the grid used here, some distortions are still seen. Therefore, we use a 10-point smoothing average to produce a smooth bed

shear stress profile.

Table 1. Summary of bedform dimensions used for the numerical experiments. For all simulations: water depth h = 8 m; mean
150   **velocity u = 0.8 m s⁻¹; bedform height H_b = 0.89 m and bedform length L_b = 24.4 m. Note that the mean lee side angle values were fixed at 5, 10, 15, 20, 25 or 30°. However, due to horizontal resolution for the sharp profile (see also Annexe A1) and the smoothing for the smooth profiles, the mean lee side angles are lower than initially set. See Figure 2 for a representation of the configurations**

<table>
<tr><td rowspan="7">Sharp profiles</td><td colspan="7" align="center">Straight lee side</td></tr>
<tr><td>Mean lee side angle (°)</td><td>5.0</td><td>9.9</td><td>14.6</td><td>19.5</td><td>24.2</td><td>28.7</td></tr>
<tr><td colspan="7" align="center">Complex lee side</td></tr>
<tr><td>Mean lee side angle (°)</td><td>4.9</td><td>10.0</td><td></td><td>20.2</td><td></td><td></td></tr>
<tr><td>Maximum lee side angle (°)</td><td>10, 25</td><td>20</td><td></td><td>30</td><td></td><td></td></tr>
<tr><td>Configurations for each maximum angle</td><td>1-4</td><td>1-4</td><td></td><td>1-4</td><td></td><td></td></tr>
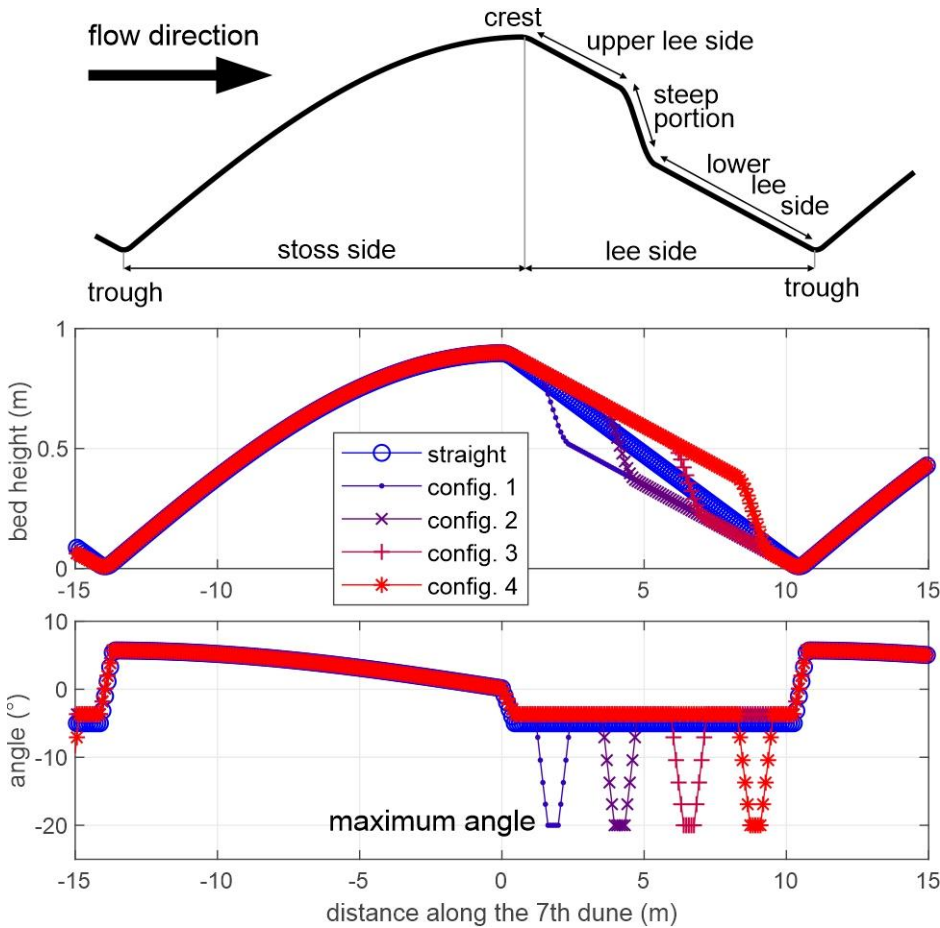<tr><td colspan="7"></td></tr>
<tr><td rowspan="6">Smooth profiles</td><td colspan="7" align="center">Straight lee side</td></tr>
<tr><td>Mean lee side angle (°)</td><td>4.9</td><td>9.3</td><td>13.5</td><td>17.5</td><td>21.2</td><td>24.7</td></tr>
<tr><td colspan="7" align="center">Complex lee side</td></tr>
<tr><td>Mean lee side angle (°)</td><td>4.9</td><td>9.4</td><td>13.7</td><td>17.5</td><td>21.2</td><td></td></tr>
<tr><td>Maximum lee side angle (°)</td><td>10, 15, 20, 25, 30</td><td>15, 20, 25, 30</td><td>20, 25, 30</td><td>25, 30</td><td>30</td><td></td></tr>
<tr><td>Configurations for each maximum angle</td><td>1-4</td><td>1-4</td><td>1-4</td><td>1-4</td><td>1-4</td><td></td></tr>
</table>

Figure 2. Example of the different configuration tested, here for a mean lee side angle of 5°, a maximum angle of 20° and a smooth profile

3 Results

The results from all the simulations (Figure 3) show that the relative flow separation length and the mean TKE generally
increase with increasing mean lee side angle. Both are linearly related to mean lee side angle: relative flow separation length
= 0.17 x mean lee side angle - 0.67 (R^2 = 0.70) and mean TKE = 0.00004 x mean lee side angle – 0.0009 (R^2 = 0.87). They
also generally increase as a function of the maximum lee side angle, but with a wide spread in the data (Figure 3b and 3e).
There does not seem to be any clear pattern which relates the flow separation length or the mean TKE to the relative position
of the maximum lee side angle (Figure 3c and 3f). The relative length of the turbulent wake shows strong variations and does
not seem to be linearly related to mean or maximum lee side angle or its position. A distinct overall trend of relative flow
separation length, TKE and relative turbulent wake length as a function of a combination of mean lee side angle and maximum
lee side angle value and position could not be identified. There is therefore is no influence of the combined mean angle and

maximum angle value and location on flow properties. The maximum TKE above the 7th dune is linearly related to the mean TKE above the 7th dune ($R^2 = 0.95$, Appendix A3). Therefore, the trends described for mean TKE are also seen for the

170   maximum TKE. Although some differences are seen between the smooth and sharp profiles, there is no systematic difference (Appendix A4).

Based on our results, we find it useful to make a distinction between low-angle dunes with mean lee side less than 10°, intermediate-angle dunes with mean lee side ca. 10° to 17°, and high-angle dunes with mean lee side more than ca. 17°. Therefore, we describe flow properties and how they are affected by the value and position of the maximum angle based on

175   these three categories in the next sections.
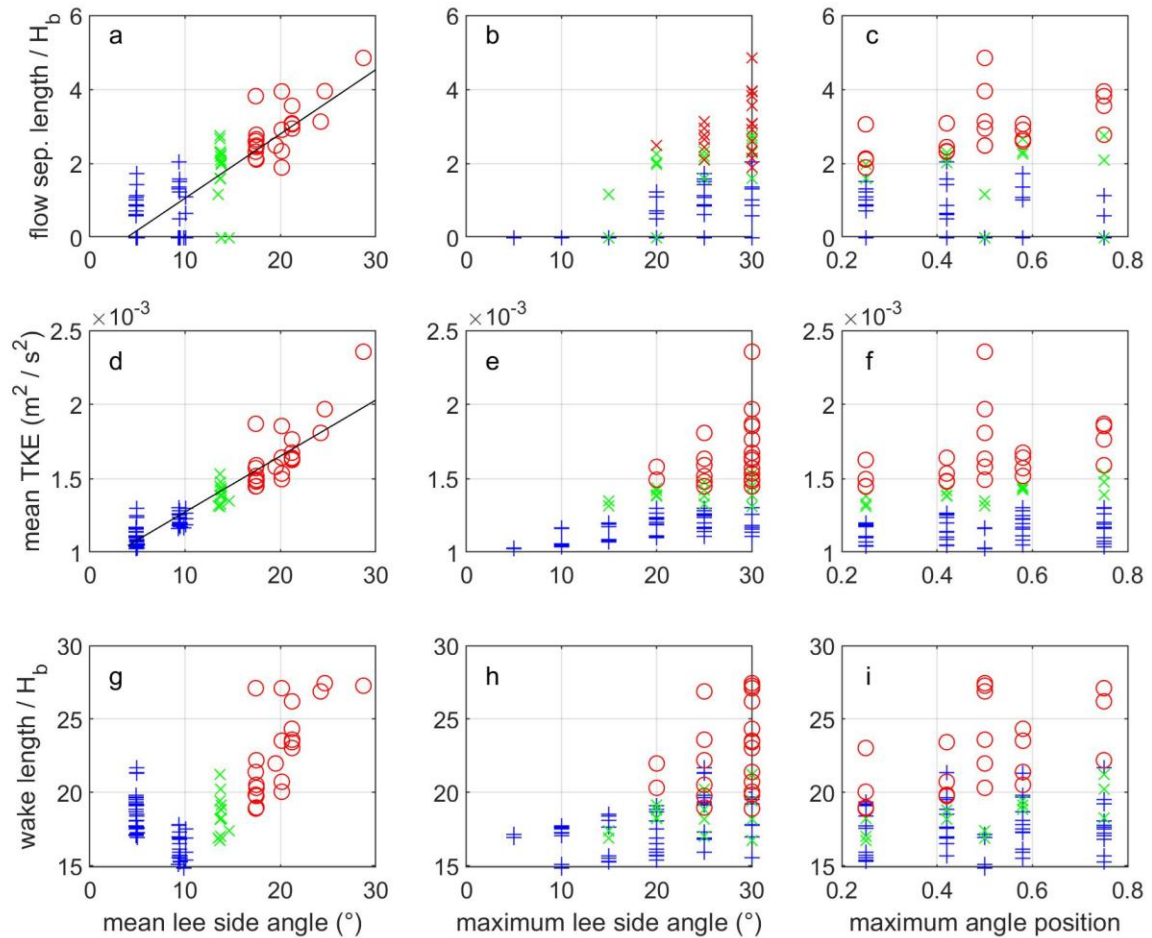
Figure 3. Relative flow separation length (flow separation length / bedform height H$_b$), mean Turbulent Kinetic Energy (TKE) and relative length of the turbulent wake (wake length / H$_b$) as a function of mean lee side angle (a, d, g), maximum lee side angle (b, e,

180   h) and the position of the maximum lee side angle (a position of 0.5 indicates a straight lee side) (c, f, i). The blue plusses show results from dunes with mean lee side lower than 10°, green crosses for mean lee sides between 10 and 17° and red circles for mean lee side > 17°

3.1 Low-angle dunes

185 Low-angle dunes (mean lee side angle < 10°) represents 89% of the dunes measured in the Weser by Lefebvre et al. (2021) and 41% of dunes measured in large rivers by Cisneros et al. (2020). Flow and turbulence patterns over low-angle dunes are illustrated by Figure 4, which shows dunes with a mean lee side of around 5° and a maximum angle of 10°, the most common configuration in the Weser Estuary. As typically observed over dunes, the horizontal velocity is highest above the crest and lowest above the trough. Vertical velocity shows downward flow above the lee side, with the strongest downward flow

190 observed above the steep portion, and upward flow above the stoss side. There is generally no flow separation over dunes with a mean lee side angle of 10° or less. However, if the maximum angle is at least 20° and situated close to the trough, a small flow separation may develop over the steep portion (Figure 5). For example, dunes with a mean lee side of 10° and a maximum lee side of 20° will not have a flow separation for config1 and config2 (where the maximum angle is positioned in the upper part of the lee side) but will have a small flow separation for config3 and config4 (where the maximum angle is positioned in

195 the lower part of the lee side). It should be noted that dunes with a lee side angle of less than 10° but a maximum lee side angle of 20° or more represents only 2.75% of all dunes measured by Cisneros et al (2020) in large rivers and 1.70% of dunes measured in the Weser Estuary by Lefebvre et al (2021). Therefore, they are not commonly observed.

Over low-angle dunes, the shear layer stays close to the bed and is the thickest above the upper lee side and the steep portion. The maximum TKE is situated close to the trough independently of the steep portion position. The turbulent wake generally

200 starts over the steep portion and extends downstream down to a distance of ca. 5 H_b after the trough. Therefore, although the mean and maximum TKE are strongest for steep portions closest to the trough, the turbulent wake is longest for steep portions close to the crest (Figure 4).
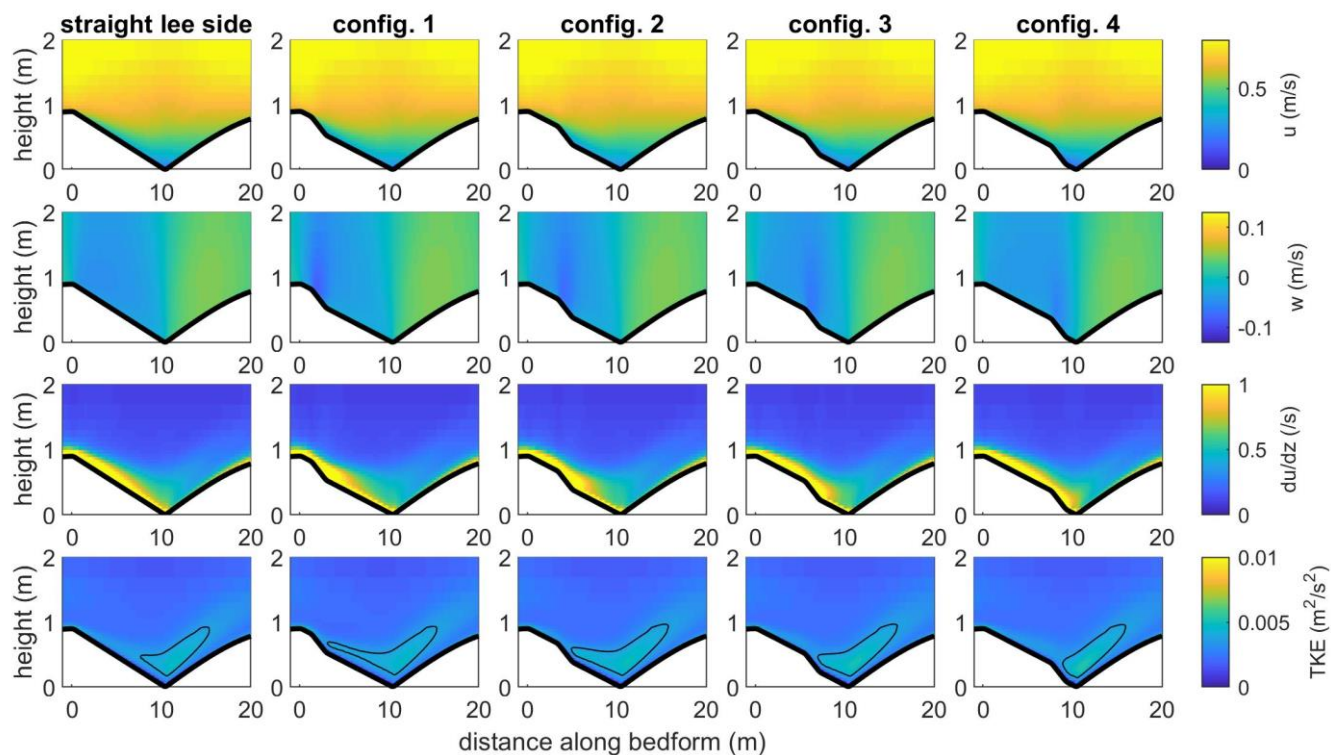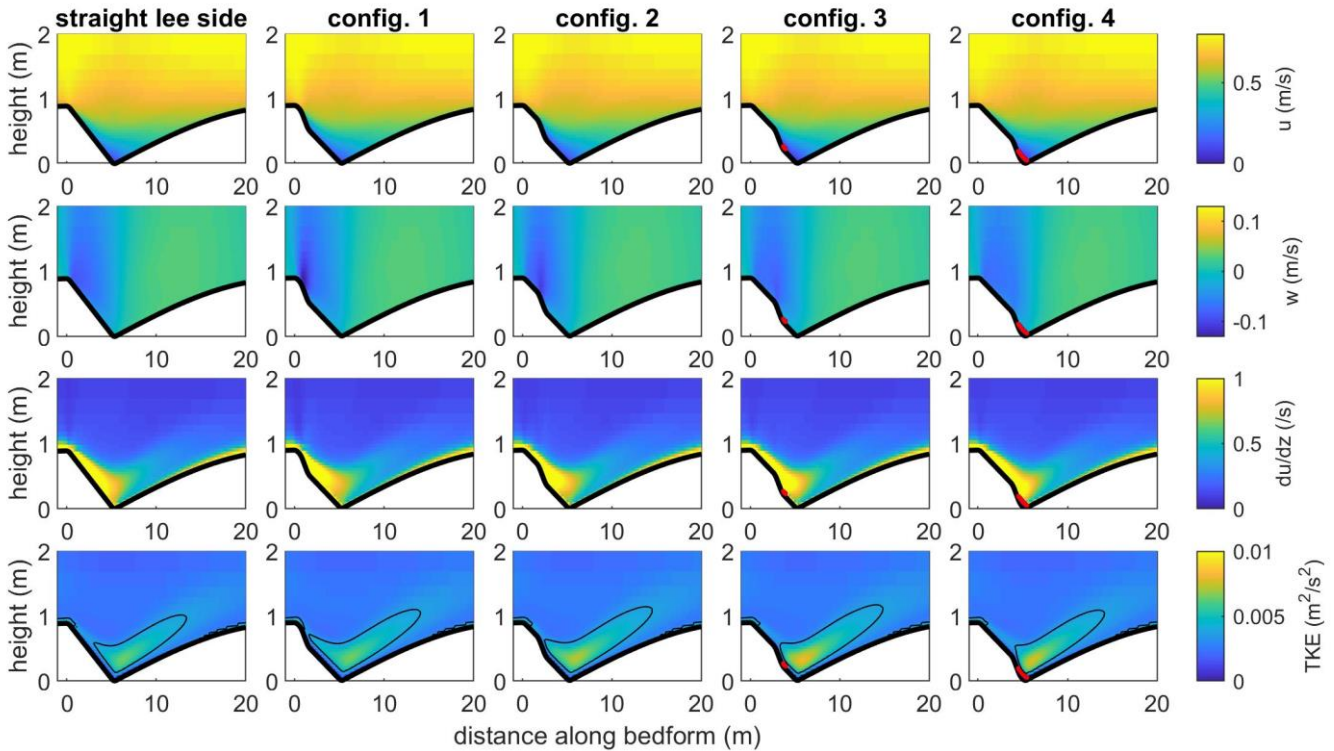
Figure 4. Horizontal and vertical velocities (u and w), vertical gradient of streamwise velocity (du/dz) and TKE above bedforms with a mean lee side of ca. 5° and maximum angle of 10°. The black lines on the bottom figures show the contour of TKE>0.0038 m²/s² to highlight the position of the turbulent wake

Figure 5. Horizontal and vertical velocities (u and w), vertical gradient of streamwise velocity (du/dz) and TKE above bedforms with
a mean lee side of ca. 10° and maximum angle of 20°. The thick red lines show the upper limit of the flow separation zone. The black
lines on the bottom figures show the contour of TKE>0.0038 m²/s² to highlight the position of the turbulent wake

3.2 Intermediate-angle dunes

Intermediate-angle dunes (defined here as mean lee side angles between 10° and 17°) represents 11% of the dunes measured
in the Weser by Lefebvre et al. (2021) and 43% of dunes measured in large rivers by Cisneros et al. (2020). From results of
simulations over intermediate-angle dunes, it is difficult to find distinctive trends in terms of the presence and size of flow
separation and TKE patterns with relation to the maximum angle value and its position. A small flow separation is generally
found, although not systematically. For example, a flow separation is often absent over dunes where the maximum angle is
close to the crest (Figure 6) and / or for sharp profiles. Interestingly, flow separation does not always start at the brink point
but is centered over the trough. As a result, the flow separation is usually longer for maximum angles close to the crest than
for maximum angles close to the trough. Over intermediate-angle dunes, the shear layer extends from the dune crest and down
the lee side reaching just above the dune trough regardless of maximum angle location. It becomes thicker moving down the
lee side until detaching near the location of flow separation. The maximum TKE is found close to the trough. The turbulent
wake is situated over the trough, independently of the maximum angle position. It is longer than over low-angle dunes, but its
size does not vary significantly depending on the position of the maximum angle for a given mean angle.
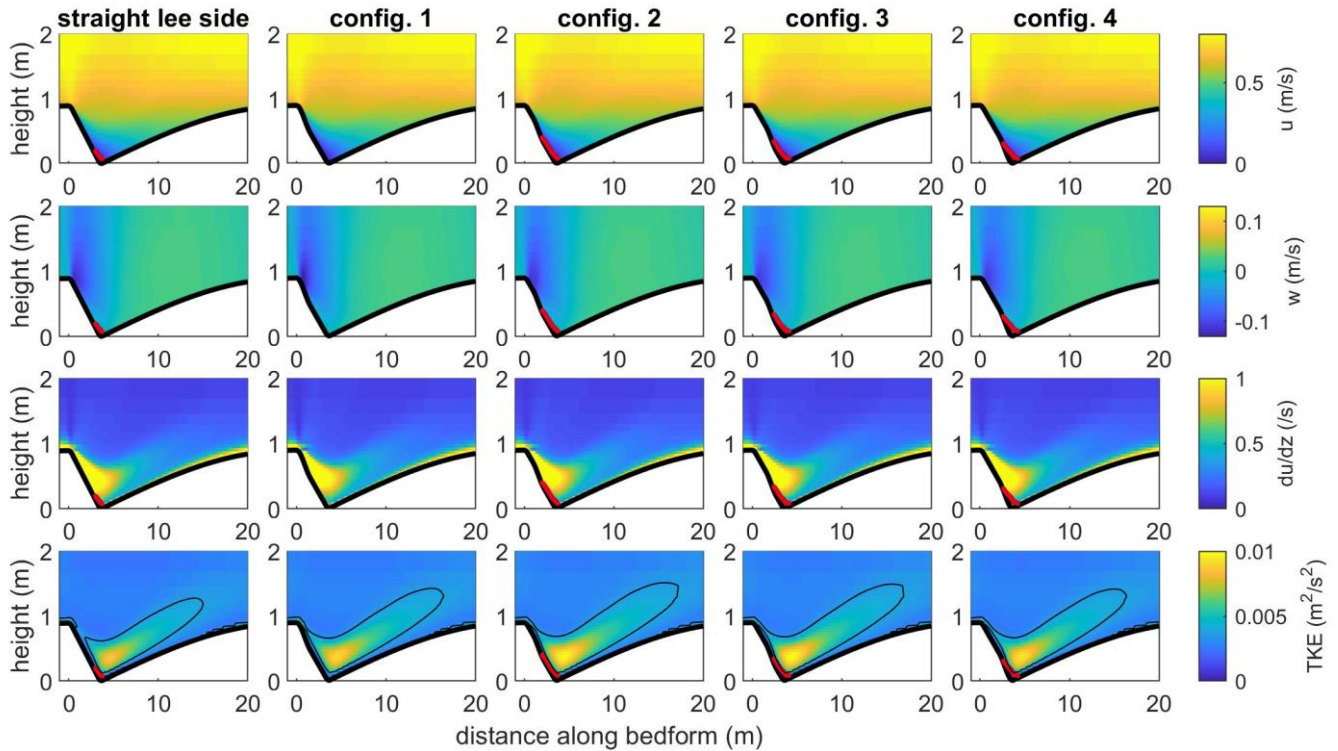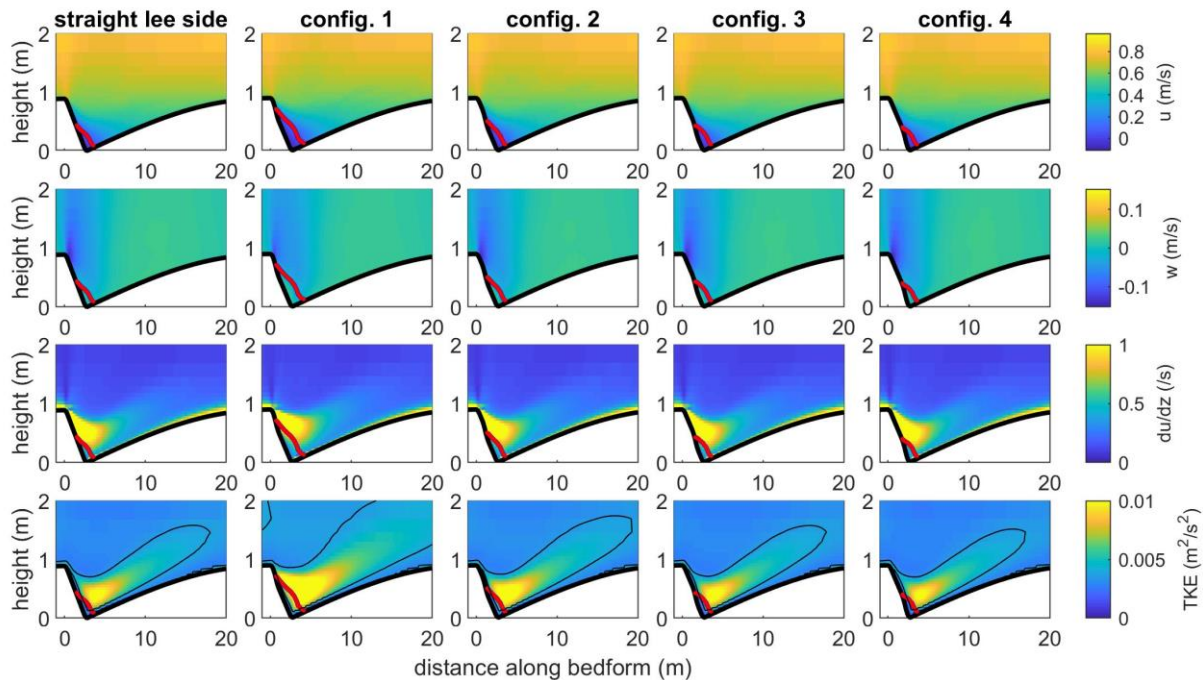
11

Figure 6. Horizontal and vertical velocities (u and w), vertical gradient of streamwise velocity (du/dz) and TKE above bedforms with a mean lee side of ca. 15° and maximum angle of 20°. The thick red lines show the upper limit of the flow separation zone. The black lines on the bottom figures show the contour of TKE>0.0038 m²/s² to highlight the position of the turbulent wake

3.3 High-angle dunes

High-angle dunes (defined here as mean lee side angles over 17°) represents only 0.03% of the dunes measured in the Weser by Lefebvre et al. (2021) and 16% of dunes measured in large rivers by Cisneros et al. (2020). A flow separation is always observed above high-angle dunes. The flow generally separates over the steep portion and reattaches shortly after the trough (Figure 7). Therefore, flow separation is longer for maximum angles situated close to the crest than for those situated close to the trough. The highest downward velocity is always situated just after the crest, independently of the maximum angle position. The shear layer detaches from the lee side shortly before flow separation. Significant differences are observed for the turbulent wake depending on the maximum angle position: it is especially strong (i.e. high TKE intensity) and spatially developed for steep portions close to the crest, so much so that a stacked wake (i.e. a turbulent wake which extends over the crest onto the next dune, as commonly observed over angle-of-repose dunes (Unsworth et al., 2018)) is seen (Figure 7). As the position of the steep portion is getting closer to the trough, the turbulent wake decreases in size and intensity.

12

Figure 7. Horizontal and vertical velocities (u and w), vertical gradient of streamwise velocity (du/dz) and TKE above bedforms with a mean lee side of ca. 20° and maximum angle of 30°. The thick red lines show the upper limit of the flow separation zone. The black lines on the bottom figures show the contour of TKE>0.0038 m²/s² to highlight the position of the turbulent wake

3.4 Bed shear stress

The bed shear stress variations above the dunes are influenced by the dune shape (Figure 8). Bed shear stress generally increases along the stoss side and reaches a maximum at the crest. It then decreases along the lee side and reaches a minimum above the trough. However, this decrease is not linear even when the lee side is straight. Instead, there is a strong decrease over the first half of the lee side, and a slower decrease or stabilisation in the lower half. It should be noted that the bed shear stress over a 30° lee side angle reaches slightly negative values (minimum value of -0.01 N m⁻² over a straight lee side) due to flow separation, but stays relatively high for a 10° lee side angle (minimum value of 0.21 N m⁻² over a straight lee side). The maximum lee side angle position has an effect which is observed mainly over low-angle lee sides. If the maximum angle is close to the crest, the bed shear stress decreases strongly over the steep portion, increases gently over the lower lee side, with a little dip over the trough and a strong increase over the stoss side. If the maximum angle is situated towards the trough, bed shear stress decreases slowly over the upper lee side before a sudden decrease over the steep portion reaching a minimum over the trough. The value of the minimum bed shear stress also varies depending on the maximum angle position. For a mean angle of around 5° and a maximum angle of 30°, minimum bed shear stress is 0.03 N m⁻² if the maximum angle is close to the

crest and -0.01 N m^{-2} if the maximum angle is close to the trough (presence of a small flow separation). Therefore, the position and value of the minimum bed shear stress is impacted by the position of the maximum angle.
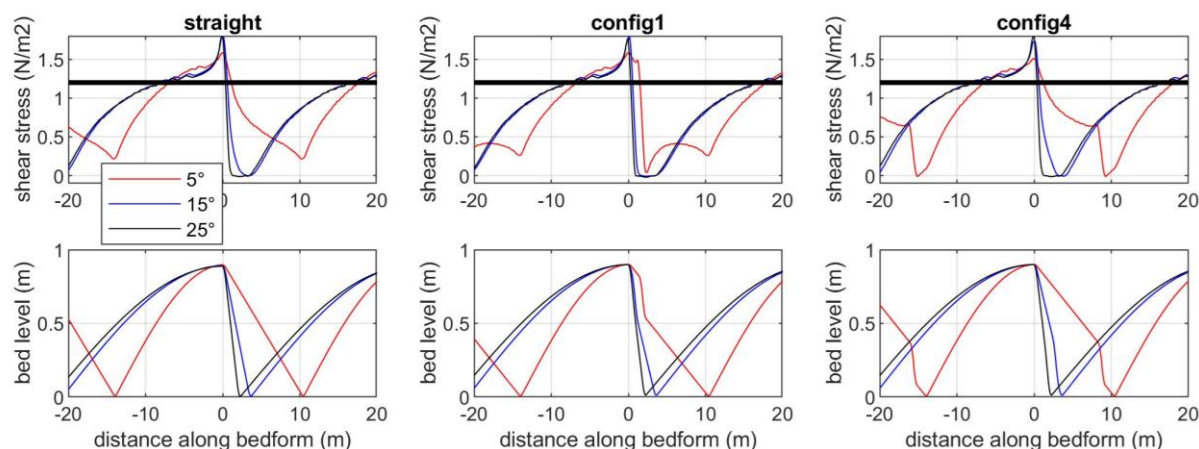

Figure 8. Bed shear stress and bed level for bedforms with a mean lee side of 5°, 15° and 25° and with a straight lee side (left panel), or a maximum angle of 30° close to the crest (config1, middle panel) or close to the trough (config4, right panel). The thick black line on the upper plots shows the critical shear stress for bed load transport

4 Discussion

4.1 Low, intermediate and high-angle dunes

Our results show that the mean lee side angle has the strongest control over flow separation and turbulence over dunes, with a secondary influence of the position and value of the maximum lee side angle depending on mean lee side angle values. Following these results, we propose a distinction between three types of dune: (1) low-angle dunes with mean lee side of less than 10°, (2) intermediate-angle dunes with mean lee side between ca. 10 and 20°, and (3) high-angle dunes with mean lee side of more than 20°. This differs from many classifications which recognise only high and low-angle dunes, sometimes without a clear definition, and do not (explicitly) recognise intermediate-angle dunes. For example, Best (2005) refers to high angle-of-repose dunes and low angle but specifying the slopes at which they are differentiated. Roden (1998) defined dunes with lee side angle > 20° as steep and lee side angle <10 as low angle dune, Kostaschuk and Villard (1996) ~~differentiates~~ differentiate symmetric dunes with mean lee side slopes < 8° and asymmetric dunes with slopes > 19° and Kostaschuk and Venditti (2019) ~~describes~~ classify high-angle dunes with lee side ~~angles~~ maximum angles > 24° and low-angle dunes with lee side ~~angles~~ maximum angles < 24° ~~but often 10°~~. These three publications therefore recognised the existence of intermediate-angle dunes but only ~~explicitly~~ implicitly. Best and Kostaschuk (2002) ~~defines~~ define low angle lee sides with slopes <10° but ~~mentions~~ mention the "transition region for the onset of flow separation (e.g., 10° − 15°)". We base our classification between low, intermediate and high-angle dunes on flow properties investigated in the

14

285 present study, ~~but also~~ on flow properties and sediment dynamics from previous research (e.g. Best and Kostaschuk, 2002;
Bradley et al., 2013; Kwoll et al., 2016; Naqshband et al., 2018; Kostaschuk and Villard, 1996). From this, some properties of
each dune category can be identified (Figure 9). Over low-angle dunes (mean lee side < 10°), there is no flow separation,
except if a very steep portion (slope > 20°) is found. Low-angle dunes generate little turbulence and are likely to induce little
bedform roughness (Lefebvre and Winter, 2016; Kwoll et al., 2016). Over intermediate dunes (mean lee side angles between

290 10° and 20°), flow separation is intermittent (Kwoll et al., 2016). Turbulence and roughness are intermediate between low and
high-angle dunes. No patterns were found between the position of the maximum angle and flow properties. Our results show
the limitations of studying intermediate dunes with Reynolds-averaged models such as Delft3D. We suggest that these dunes
should be investigated with laboratory experiments, field measurements and Reynolds-resolving models in order to precisely
characterise the case of intermittent flow separation where little information is known. Over high-angle dunes (mean lee side

295 > 20°), a developing to fully developed flow separation is present, a strong turbulent flow is observed and a high bedform
roughness is created. If the maximum angle is close to the crest, flow separation is longer and the turbulent wake is stronger
than if the maximum angle is close to the trough.
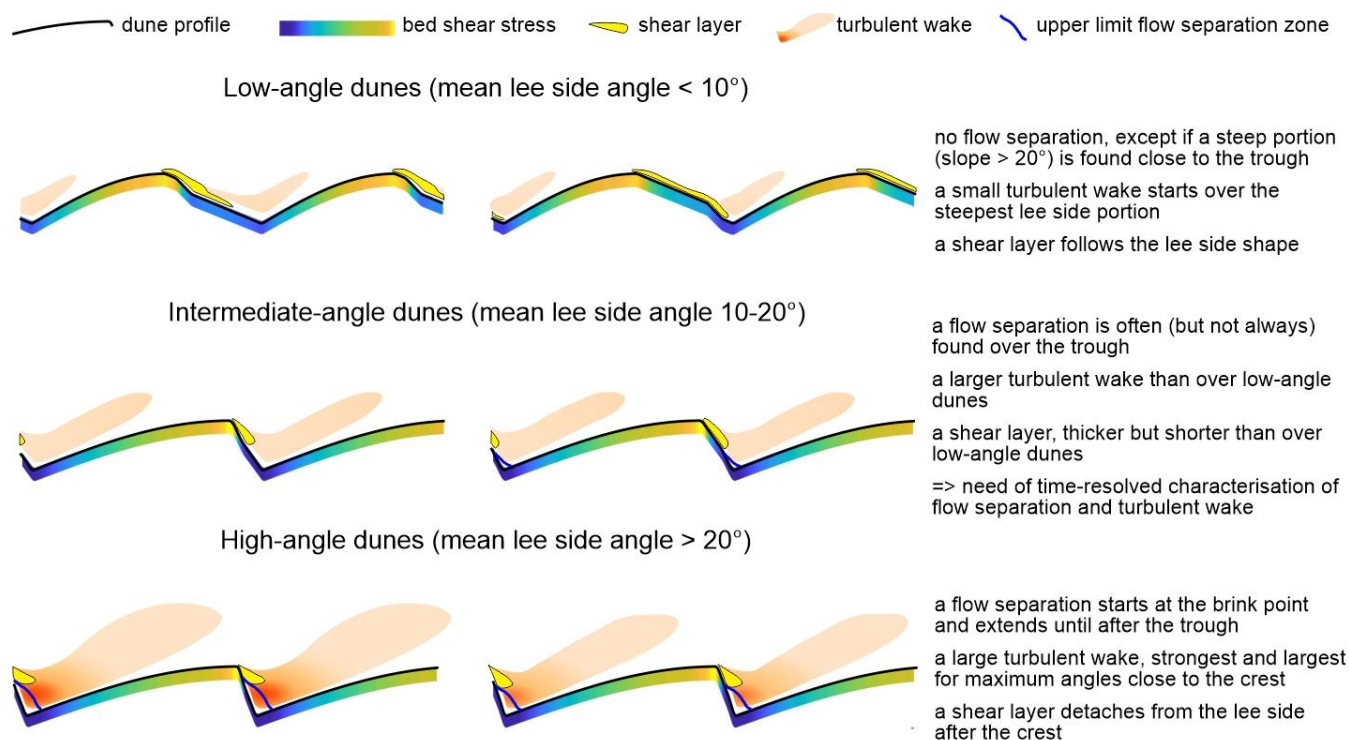
Figure 9. Summary of the results showing the main characteristics of flow over low-angle, intermediate-angle and high-angle dunes

15

The distinction that we give here of 20° between intermediate and low-angle dunes differs lightly from that which we used in the results section, 17°. That is because flow separation over dunes with lee sides less than 20° is still small compared to a fully developed flow separation and these dunes might still classify as intermediate dunes. Furthermore, the mean lee side

305 separating intermediate and high-angle dunes might vary depending on relative dune height (dune height compared to water depth; Lefebvre and Winter, 2016). More research on intermediate dunes might help determine precisely the separation between intermediate and high-angle dunes. In any case, there is probably not an exact value but a range of mean lee side angles showing the transition between each dune category depending on the specific hydrodynamic conditions.

This distinction between low, intermediate and high-angle dunes is important for a range of processes, for example the

310 evaluation of bed roughness, understanding the relation between hydrodynamics, sediment transport, and dune morphology, how dunes are identified in the depositional record, and unravelling the controlling processes leading to different lee side angle slopes and shapes.

4.2 Lee side morphology

315 We investigated the influence of "complex" dune morphologies, still simplified as three portions, but with a maximum angle placed towards the crest (creating a sharp crest) or placed towards the trough (creating a rounded crest). Dunes in rivers are predominantly low to intermediate-angle dunes with a rounded crest (Cisneros et al., 2020) and are similar to the config3 and config4 morphologies, which means that flow over river dunes will likely follow the results observed over those configurations. Following this assumption, river dunes, in general, are likely to have no or intermittent flow separation and a relatively strong

320 contained over the trough. The bed shear stress will be slowly decreasing over the upper lee side and strongly decreasing over the steep portion.

Dunes in estuaries are predominantly low-angle dunes with a sharp crest (Lefebvre et al., 2021; Dalrymple and Rhodes, 1995) so they will mainly follow the results from config1 and config2. Following the modelled results over these lee side morphologies, it is unlikely that there is a permanent flow separation for low-angle sharp crested dunes. The turbulence will

325 be low and diffused along a large, long turbulent wake with low TKE. The bed shear stress will have a strong decrease over the upper part of the lee side and then be stable or increase slightly over the lower lee side.

Dunes on the continental shelf may have any type of morphology ~~going~~ from sharp to round crested (Van Landeghem et al., 2009; Zhang et al., 2019). The shape of marine dunes is likely to reflect the local conditions of hydrodynamics and sediment transport. For example, a strongly asymmetric dune with a flat crest may form in an environment where the tidal currents are

330 strongly asymmetrical. Large symmetrical dunes with sharp crests will develop in environments with symmetrical or weakly asymmetrical currents and ample sand supply (Ma et al., 2019). Our results show that the dune shape will affect how they interact with the flow. However, so far, the precise mean and maximum angles and the detailed shape (e.g. position of maximum angle) has been systematically quantified only for large rivers and the Weser Estuary. Therefore, it is essential that the lee side shape is characterised with a precise determination of mean and maximum angles, ~~and~~ the position of the maximum

16

335 angle, ~~also possibly~~ *and* the size and location of the steep portion in order to precisely understand and predict the complex interaction between hydrodynamics, sediment transport and bed morphology. Since high-resolution multibeam data are now routinely collected during surveys, it can and should be routinely done.

In this study, we have assumed that there was only one scale of dunes. However, compound bedforms are often observed, with smaller bedforms superimposed on larger ones, usually over the stoss side. When the lee side of large dunes is low, secondary

340 bedforms may also be found over the lee side (Zomer et al., 2021). These secondary bedforms can have a strong influence on flow above dunes, as even if the primary dune mean lee side angle is low, the lee side of the secondary bedforms may be steep and therefore, flow separation and roughness will be created over such compound dunes. The simulations with mean lee side 5° and maximum lee side >20° certainly show the possibility for permanent flow separation over such low-angle primary dunes if there are some steep secondary bedforms. This has the potential to create high roughness as the wakes are mixing

345 with one another when they are advecting downstream in the case that several steep secondary bedforms are found on the lee side of low-angle primary dunes. Further studies could therefore investigate the interaction between the turbulence and flow separation of the secondary bedforms found over low-angle dunes. However, this does require high-spatial resolution for the secondary bedforms to be properly resolved and, if the experiments are carried out with moving sediment, the temporal scales required to observe this interaction would be related to the rate of superimposed bedform migration.

350

4.3 Potential impact on bedform roughness

Bedform roughness varies depending on lee side angle (Kwoll et al., 2016; Lefebvre and Winter, 2016). In the present study, we could not quantify directly the variations in roughness. However, bedform roughness is related to turbulence intensity over dunes (Lefebvre et al., 2016). Here, we observe that mean and maximum turbulence generally increases with increasing mean

355 lee side angle. However, for the same mean lee side angle, there are still variations in turbulence created by the value and position of the maximum slope (Figure 3). This means that bedform roughness is likely to be affected not only by the mean lee side angle, but also by the value and position of the maximum angle. However, no practical way has been found to characterise the roughness of low-angle dunes, and a definite relation between lee side angle of natural dune field and roughness has not yet been established. For example, no relation was found between dune lee properties and roughness

360 variations in the river Waal in the Netherlands (De Lange et al., 2021). Therefore, it currently seems unlikely that the effect of the value and position of the maximum lee side angle can easily be considered when estimating bedform roughness of a natural bedform field. Instead, research should focus on relating bedform statistical properties, ~~for example~~ *such as* the integrated slope area, ~~to~~ roughness measurements in the field, and developing practical ways to incorporate these in model simulations. Indeed, bedform roughness variations due to bedform asymmetry has a strong impact on velocities and bedload transport calculation

365 in tidal environments (Herrling et al., 2021)

4.4 Potential impact on sediment transport

The variation of bed shear stress across different dune morphologies will impact the potential for sediment transport. The extended area of critical bed shear stresses near the crest of the dune in config1 (maximum angle near the crest) implies that

370 there is higher ability of sediment to be transported from the dune crest in these configurations compared to the rounded crest (config4) cases for low-angle (5°) dunes. Alternatively, there is very little difference in the bed shear stress curves for the high-angle lee side case, which implies that the sediment transport potential for the different dune morphologies will be less impacted by the location of a steep slope in these high-angle cases. The difference between the shear stress curves from the low to the high-angle cases require [requires] that we account for the spatial variations in bed shear stress across the dune to better

375 understand the sediment transport potential in these systems and the likely bedform evolution that will occur from these different bed shear stress patterns.

The differences in bed shear stress curves for the low-angle dunes are related to variations in velocity magnitude above the lee side, which can also be recognised in the shapes of the shear layer and turbulent wake. In the case when the steep portion is close to the crest, there is a rapid decrease in velocity above the steep face, a thick shear layer, and the start of the turbulent

380 wake. This results in a sudden drop in bed shear stress above the upper lee side, with the minimum shear stress found over the steep portion and a higher bed shear stress found over the lower lee side with a second minimum over the trough. In the case when the steep portion is close to the trough, there is a gradual decrease in velocity along the long and gently sloping upper lee side, a thin shear layer, and the turbulent wake is situated over the trough. This results in a gradual lowering of the bed shear stress until it reaches its minimum over the steep face close to the trough. This shows the ways the differing flow

385 dynamics and wake regions over complex lee side shapes may influence the along stream bed shear stress and resultant sediment transport across low-angle dunes.

5 Conclusions

Numerical simulations were carried out in order to estimate the influence of the value and position of the maximum lee side

390 angle on flow above dunes with varied mean lee side slopes. Based on our results and previous literature, we propose a distinction between three types of dunes:

Low-angle dunes, with mean lee side slopes lower than 10°. Over such dunes, there is no permanent flow separation, except if the maximum angle is more than 20° and close to the through. The turbulent wake is generally weak, but strongest and most contained [compact] (limited spatial extent) for steep maximum angles situated close to the trough. The variations in velocity magnitude

395 and turbulence intensity along the dune influence the bed shear stress and potential for sediment transport across different lee side shapes.

18

Intermediate-angle dunes, with mean lee side of 10 to 20°. Over such dunes, there is rarely a permanent flow separation but it is likely that an intermittent flow separation forms. When present, flow separation is observed over the trough, independently of the maximum lee side angle position. These dunes should be studied systemically and in detail with laboratory experiments and eddy-resolving numerical modelling.

High-angle dunes, with mean lee side of more than 20°. Over such dunes, the flow separates at, or just downstream of, the brink point and therefore, flow separation is longest if the maximum angle is close to the crest. The turbulent wake is strong, and extensive strongest and most extended for steep maximum slopes situated close to the crest.

The This classification scheme introduced herein is more specific than previous classification schemes, which only introduced considered low and high-angle dunes, and describes the specifics of flow properties depending on that are controlled by lee side morphology. Importantly, this new classification scheme for dune lee sides It allows for a precise consideration of the interaction between dune morphology and flow. To correctly take this interaction and its consequences into account, detailed reports of dune morphology from varied environments are needed.

Appendix

Appendix A – extra figures

Appendix A1: comparison of flow and turbulence over flat bed and straight angle-of-repose dunes
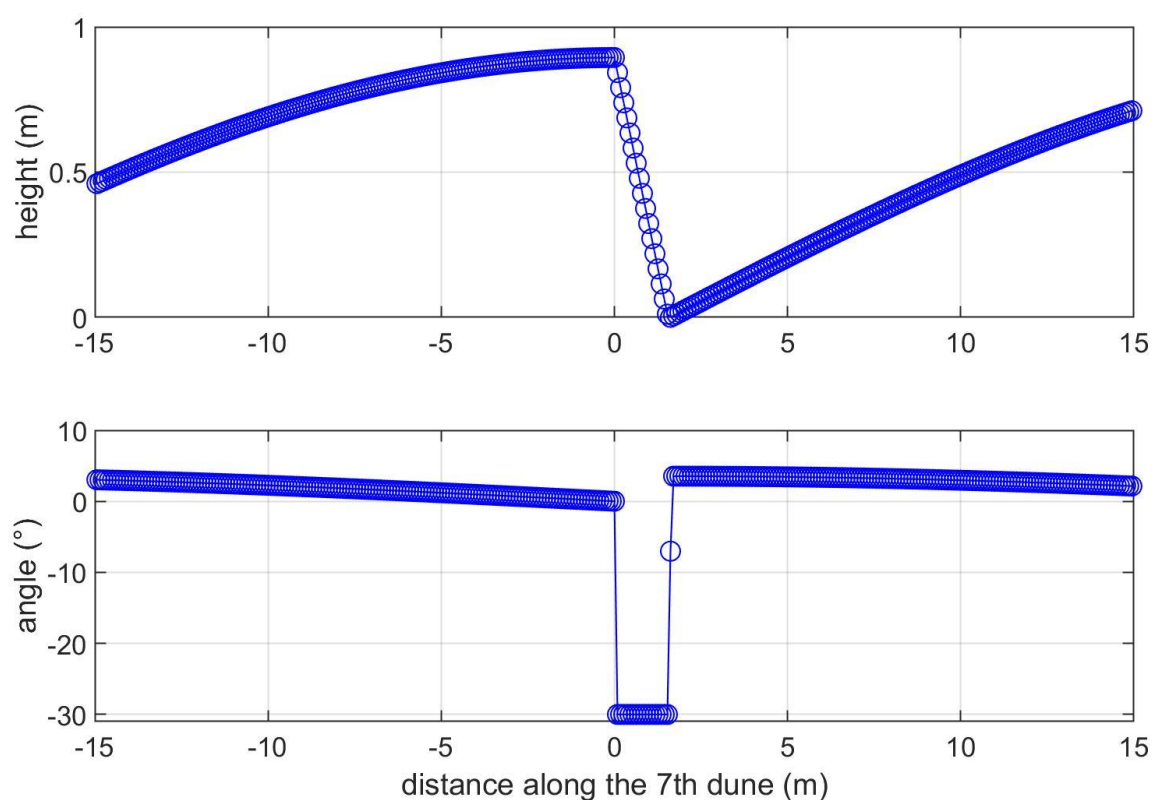

430

Figure A1. Example of a straight lee side configuration. Because of the need to define the bedform profile on the grid, the last lee side angle is not 30° but ca. 8°, and therefore, the mean lee side angle is 28.7° instead of 30°

435

A2. Comparison of mean and maximum TKE over the 7th bedform for all the experiments

The maximum and mean TKE above the 7th bedform are linearly related:

Max. TKE = 12.4581 x mean TKE - 0.0079, R^2 = 0.95, number of points = 88.
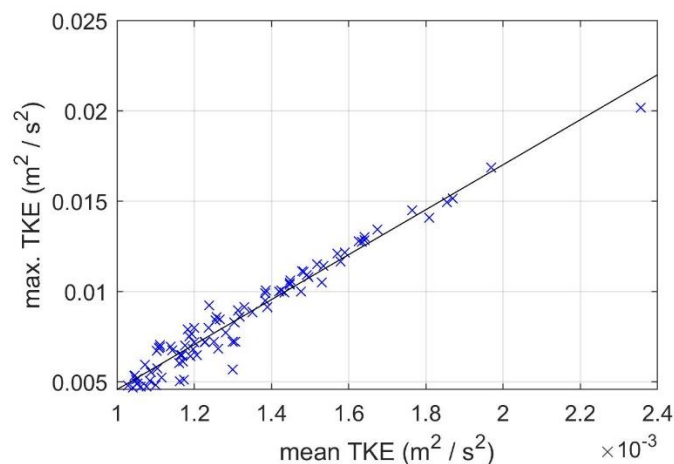
Figure A2. Mean and maximum TKE above the 7th bedform for all the simulations

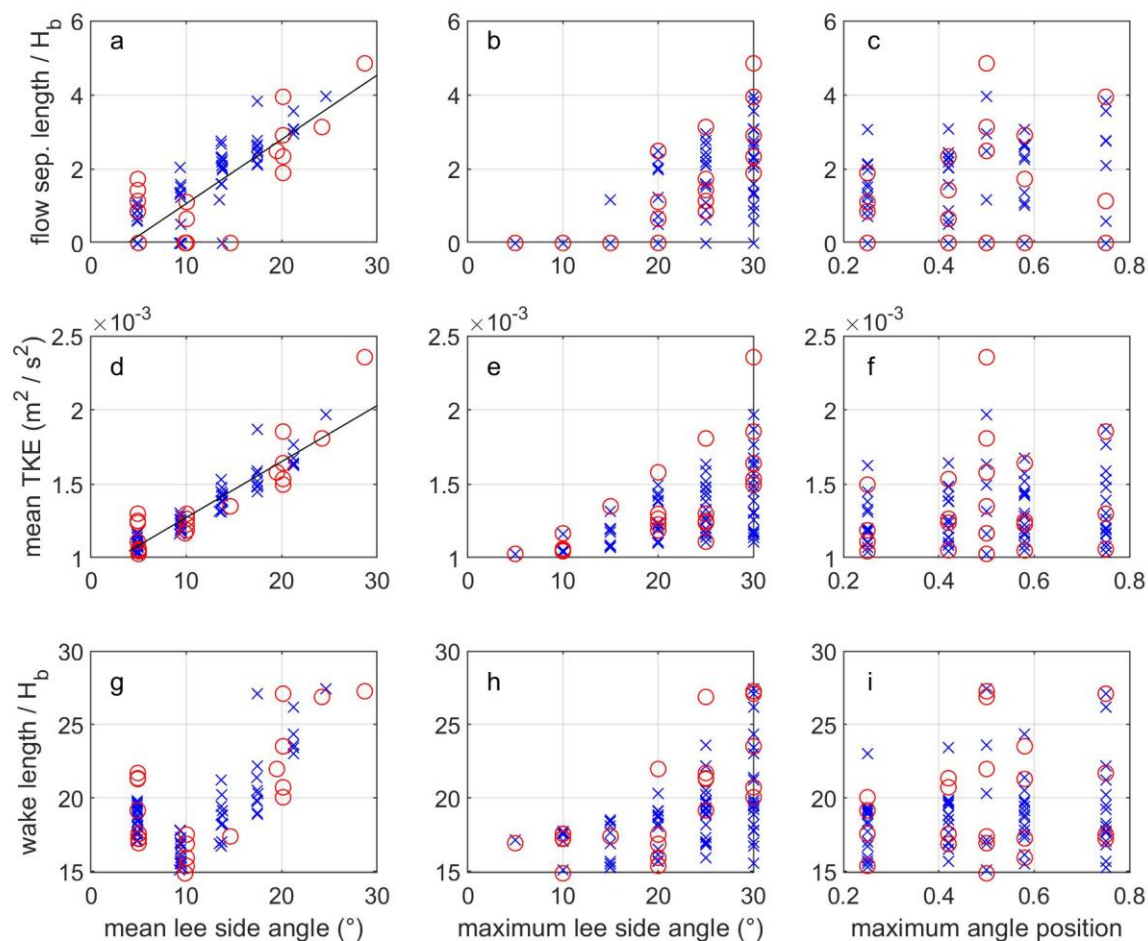## A3. Comparison of properties over smooth and sharp lee sides

465

Figure A3. Relative flow separation length (flow separation length / bedform height H_b), mean Turbulent Kinetic Energy (TKE) and relative length of the turbulent wake (wake length / H_b) as a function of mean lee side angle (a, d, g), maximum lee side angle (b, e, h) and the position of the maximum lee side angle (a position of 0.5 indicates a straight lee side) (c, f, i). This figure is similar to Figure 3 from the main manuscript but the properties calculated from the sharp dunes are plotted in red

470   circles and those from the smooth dunes in blue crosses in order to highlight the lack of systematic differences.

Code availability

Data availability

The main results will be made available through https://www.pangaea.de/ as soon as the manuscript is accepted with minor revisions. Pangaea is a Data Publisher for Earth & Environmental Science where data can be archived, published, and re-used following FAIR principles. For now, the data are uploaded as an excel document as the data may still change during the review process.

Author contribution

AL and JC conceptualised the study and planned the experiments; AL performed and analysed the numerical simulations; Experimental results were discussed by AL and JC; the original draft was prepared by AL and commented by JC; further writing, review and editing were done by AL and JC.

Competing interests:

The authors declare that they have no conflict of interest.

Acknowledgements

References

Bennett, S. J. and Best, J. L.: Mean flow and turbulence structure over fixed, two-dimensional dunes: implications for sediment transport and bedform stability, Sedimentology, 42, 491-513, https://doi.org/10.1111/j.1365-3091.1995.tb00386.x, 1995.

Best, J.: The fluid dynamics of river dunes: A review and some future research directions, J. Geophys. Res., 110, 21, https://doi.org/10.1029/2004JF000218, 2005.

Best, J. and Kostaschuk, R.: An experimental study of turbulent flow over a low-angle dune, J. Geophys. Res., 107, 3135, https://doi.org/10.1029/2000JC000294, 2002.

Bradley, R. W., Venditti, J. G., Kostaschuk, R., Church, M. A., Hendershot, M., and Allison, M. A.: Flow and sediment suspension events over low-angle dunes: Fraser Estuary, Canada, J. Geophys. Res., 118, 1693-1709, https://doi.org/10.1002/jgrf.20118, 2013.

Cisneros, J., Best, J., van Dijk, T., de Almeida, R. P., Amsler, M., Boldt, J., Freitas, B., Galeazzi, C., Huizinga, R., Ianniruberto, M., Ma, H. B., Nittrouer, J. A., Oberg, K., Orfeo, O., Parsons, D., Szupiany, R., Wang, P., and Zhang, Y. F.: Dunes in the world's big rivers are characterized by low-angle lee-side slopes and a complex shape, Nat. Geosci., 13, 156-+, https://doi.org/10.1038/s41561-019-0511-7, 2020.

Dalrymple, R. W. and Rhodes, R. N.: Chapter 13 Estuarine Dunes and Bars, in: Dev. Sedimentol., edited by: Perillo, G. M. E., Elsevier, 359-422, 1995.

de Lange, S. I., Naqshband, S., and Hoitink, A. J. F.: Quantifying Hydraulic Roughness From Field Data: Can Dune Morphology Tell the Whole Story?, Water Resour. Res., 57, e2021WR030329, https://doi.org/10.1029/2021WR030329, 2021.

Deltares: User Manual Delft3D-FLOW, Deltares, Delft, The Netherlands2014.

Franzetti, M., Le Roy, P., Delacourt, C., Garlan, T., Cancouët, R., Sukhovich, A., and Deschamps, A.: Giant dune morphologies and dynamics in a deep continental shelf environment: Example of the banc du four (Western Brittany, France), Mar. Geol., 346, 17-30, https://doi.org/10.1016/j.margeo.2013.07.014, 2013.

Herrling, G., Becker, M., Lefebvre, A., Zorndt, A., Kramer, K., and Winter, C.: The effect of asymmetric dune roughness on tidal asymmetry in the Weser estuary, Earth Surf. Processes Landforms, 18, https://doi.org/10.1002/esp.5170, 2021.

Kostaschuk, R. and Villard, P.: Flow and sediment transport over large subaqueous dunes: Fraser River, Canada, Sedimentology, 43, 849-863, https://doi.org/10.1111/j.1365-3091.1996.tb01506.x, 1996.

Kostaschuk, R. A. and Venditti, J. G.: Why do large, deep rivers have low-angle dune beds?, Geology, 47, 919-922, https://doi.org/10.1130/g46460.1, 2019.

Kwoll, E., Venditti, J. G., Bradley, R. W., and Winter, C.: Flow structure and resistance over subaquaeous high- and low-angle dunes, Journal of Geophysical Research: Earth Surface, 121, 545-564, https://doi.org/10.1002/2015JF003637, 2016.

Lefebvre, A. and Winter, C.: Predicting bed form roughness: the influence of lee side angle, Geo-Mar. Lett., 36, 121-133, https://doi.org/10.1007/s00367-016-0436-8, 2016.

Lefebvre, A., Paarlberg, A. J., and Winter, C.: Flow separation and shear stress over angle of repose bedforms: a numerical investigation, Water Resour. Res., 50, 986-1005, https://doi.org/10.1002/2013WR014587, 2014a.

Lefebvre, A., Paarlberg, A. J., and Winter, C.: Characterising natural bedform morphology and its influence on flow, Geo-Mar. Lett., 36, 379–393, https://doi.org/10.1007/s00367-016-0455-5, 2016.

Lefebvre, A., Paarlberg, A. J., Ernstsen, V. B., and Winter, C.: Flow separation and roughness lengths over large bedforms in a tidal environment: a numerical investigation, Cont. Shelf Res., 91, 57-69, https://doi.org/10.1016/j.csr.2014.09.001, 2014b.

Lefebvre, A., Herrling, G., Becker, M., Zorndt, A., Krämer, K., and Winter, C.: Morphology of estuarine bedforms, Weser Estuary, Germany, Earth Surf. Processes Landforms, https://doi.org/10.1002/esp.5243, 2021.

Ma, X., Yan, J., Song, Y., Liu, X., Zhang, J., and Traykovski, P. A.: Morphology and maintenance of steep dunes near dune asymmetry transitional areas on the shallow shelf (Beibu Gulf, northwest South China Sea), Mar. Geol., 412, 37-52, https://doi.org/10.1016/j.margeo.2019.03.006, 2019.

Maddux, T. B., Nelson, J. M., and McLean, S. R.: Turbulent flow over three-dimensional dunes: 1. Free surface and flow response, Journal of Geophysical Research: Earth Surface, 108, https://doi.org/10.1029/2003JF000017, 2003.

McLean, S. R., Nelson, J. M., and Wolfe, S. R.: Turbulence structure over two-dimensional bed forms: Implications for sediment transport, J. Geophys. Res., 99, 12729-12747, https://doi.org/10.1029/94JC00571, 1994.

McLean, S. R., Wolfe, S. R., and Nelson, J. M.: Spatially averaged flow over a wavy boundary revisited, J. Geophys. Res., 104, 15743-15753, https://doi.org/10.1029/1999JC900116, 1999.

Naqshband, S., Ribberink, J., and Hulscher, S.: Using both free surface effect and sediment transport mode parameters in defining the morphology of river dunes and their evolution to upper stage plane beds, J. Hydraul. Eng., 140, 06014010, https://doi.org/10.1061/(ASCE)HY.1943-7900.0000873, 2014.

Naqshband, S., Wullems, B., de Ruijsscher, T., and Hoitink, T.: Experimental investigation of low-angle dune morphodynamics, E3S Web Conf., 40, https://doi.org/10.1051/e3sconf/20184002056 2018.

Nelson, J. M., McLean, S. R., and Wolfe, S. R.: Mean flow and turbulence fields over two-dimensional bed forms, Water Resour. Res., 29, 3935-3953, https://doi.org/10.1029/93WR01932, 1993.

Platzek, F. W., Stelling, G. S., Jankowski, J. A., and Pietrzak, J. D.: Accurate vertical profiles of turbulent flow in z-layer models, Water Resour. Res., 50, 2191-2211, https://doi.org/10.1002/2013WR014411, 2014.

555   Prokocki, E. W., Best, J. L., Perillo, M. M., Ashworth, P. J., Parsons, D. R., Sambrook Smith, G. H., Nicholas, A. P., and Simpson, C. J.: The morphology of fluvial-tidal dunes: Lower Columbia River, Oregon/Washington, USA, Earth Surf. Processes Landforms, 47, 2079-2106, https://doi.org/10.1002/esp.5364, 2022.

Roden, J. E.: The sedimentology and dynamics of mega-dunes, Jamuna River, Bangladesh, Ph.D., Department of Earth Sciences, University of Leeds, Leeds, UK, 310 pp., 1998.

560   Uittenbogaard, R., van Kester, J., and Stelling, G.: Implementation of three turbulence models in 3D-TRISULA for rectangular grids, Tech. Rep. Z81, WL | Delft Hydraulics, Delft, The Netherlands., 1992.

Unsworth, C. A., Parsons, D. R., Hardy, R. J., Reesink, A. J. H., Best, J. L., Ashworth, P. J., and Keevil, G. M.: The Impact of Nonequilibrium Flow on the Structure of Turbulence Over River Dunes, Water Resour. Res., 54, 6566-6584, https://doi.org/10.1029/2017WR021377, 2018.

565   Van der Mark, C. F., Blom, A., and Hulsher, S. J. M. H.: Quantification of variability in bedform geometry, J. Geophys. Res., 113, F03020, https://doi.org/10.1029/2007JF000940, 2008.

Van Landeghem, K. J. J., Wheeler, A. J., Mitchell, N. C., and Sutton, G.: Variations in sediment wave dimensions across the tidally dominated Irish Sea, NW Europe, Mar. Geol., 263, 108-119, https://doi.org/10.1016/j.margeo.2009.04.003, 2009.

Venditti, J. G.: Turbulent flow and drag over fixed two- and three-dimensional dunes, J. Geophys. Res., 112, F04008, 570   https://doi.org/10.1029/2006JF000650, 2007.

Wiberg, P. L. and Nelson, J. M.: Unidirectional flow over asymmetric and symmetric ripples, Journal of Geophysical Research: Oceans, 97, 12745-12761, https://doi.org/10.1029/92JC01228, 1992.

Zhang, H., Ma, X., Zhuang, L., and Yan, J.: Sand waves near the shelf break of the northern South China Sea: morphology and recent mobility, Geo-Mar. Lett., 39, 19-36, https://doi.org/10.1007/s00367-018-0557-3, 2019.

575   Zomer, J. Y., Naqshband, S., Vermeulen, B., and Hoitink, A. J. F.: Rapidly Migrating Secondary Bedforms Can Persist on the Lee of Slowly Migrating Primary River Dunes, Journal of Geophysical Research: Earth Surface, 126, e2020JF005918, https://doi.org/doi.org/10.1029/2020JF005918, 2021.